**ORIGINAL PAPER**

# Evaluation of increasing service life of epoxy zinc-rich coating on 3 wt.% Ni-advanced low-alloy steel in marine atmospheric environment

Sheng-rong Wang[1,2] · Jian-wei Yang[1,2] · Jian-ping Cao[1,2] · Shan Jiang[1,2] · Fei-fan Xu[1,2]

**Abstract**

The addition of Ni element into steel to prolong the service life of coated steel was investigated in marine atmospheric environment by laboratory simulated accelerated experiment. The scanning electron microscope and electron probe micro-analysis combined with electrochemical impedance spectroscopy were used to characterize coated steel properties and examined the anti-corrosion performance. The results showed that 3 wt.% Ni-advanced steel (3Ni steel) substrate obviously delayed the failure time of coating compared to carbon steel, therefore prolonging the service life of coating on the steel. X-ray diffraction patterns for the corrosion products under the scratched coating on 3Ni steel exhibited that $FeNi_2O_4$ and $Fe_2O_3$ occurred in the corrosion product of 3Ni steel. It was also found that Ni element enriched in the product layer through analyzing the appearance and composition of corrosion products by electron probe micro-analysis. Chloride ions were blocked out of product by the enrichment of Ni element in rust layer.

**Keywords** 3 wt.% Ni-advanced low-alloy steel · Coating failure · Service life · Corrosion product · Marine atmosphere

## 1 Introduction

Weathering steels (WS) are usually referred to low-alloy steel and the steels with low content of carbon, and addition of one or several low/medium other alloying elements including Cu, Cr, Ni, P, etc. The total alloying content should be at least 1.00 wt.% and no more than 5.00 wt.%. WS are mainly used for applications including bridges, load-bearing structures, transmission towers, building constructions, artistic and decorative features, etc. [1, 2]. Researchers have found that the addition of alloying elements can greatly change the protection of corrosion product layer of WS, and thus it has higher corrosion resistance in urban, rural, and industrial atmosphere than carbon steel (CS) [3–6]. Moreover, in recent years, an increasing number of WS are used in coastal structures, including railway vehicles, bridges, and containers, and

others [7–9]. According to the research, Ni is specifically introduced into WS to develop a new type of steel in order to prolong the service life of steel structures in marine atmospheres, i.e., Ni-advanced WS (NAWS), which has better corrosion resistance in marine atmospheres [10–13].

In recent years, Ni has been researched as alloying element to improve corrosion resistance of WS in marine environment and the results have shown the obvious benefit effect on its performance [14–17]. However, two primary problems remained: the optimum content of Ni in WS and the mechanism of increasing corrosion resistance of WS by adding Ni. Cheng et al. [18] found that WS with 1.2 wt.% Ni has a lower corrosion rate in a simulated marine atmosphere due to the improved composition in corrosion product film. Diaz et al. [19] studied the corrosion product films of WS containing 0.92, 1.69 and 2.83 wt.% Ni formed in marine atmospheres, and it was found that the corrosion rate decreased with the increase in Ni content. Other researchers [20–22] further confirmed this conclusion and showed that the ratio of α-FeOOH was improved by the addition of Ni in corrosion product film and effectively enhanced the compactness of corrosion product. Cheng et al. [23] concluded that the optimal content of Ni in WS was approximately 3.0%–3.5%, which can provide the best

✉ Sheng-rong Wang
wangshengrong@126.com

1  Shougang Research Institute of Technology of Shougang Group Co., Ltd., Beijing 100043, China

2  Beijing Key Laboratory of Green Recyclable Process for Iron & Steel Production Technology, Beijing 100043, China

balance between the cost and corrosion protection in harsh atmosphere conditions.

WS can be used without painting due to protective rusts formed on the surface. Protective rusts are formed in natural atmospheric environments which provide excellent corrosion resistance of WS. However, conventional WS cannot be used without painting in the aggressive marine atmospheres because of porous and non-adhesive rusts formed on the steel surface. Thus, WS need be painted in the aggressive coastal marine atmosphere. Travassos et al. [24] suggested that applying unpainted WS in highly corrosive environments is impractical. WS without painting can only be used when exposed to low-corrosivity environments. The adhesion between the coating and the substrate was reduced for the increase in corrosion products of the base metal whose coating was destroyed. Therefore, it is obviously effective to use incorruptible substrate of WS for prolonging the life of coating. According to Sun et al. [25], it has been pointed that painted WS structures owned longer service life than painted carbon steel structures. Coatings are one of the most economic performance to protect steel surface against attacking from aggressive species [26–31]. The protection behavior of the coating is mainly dependent on the atmospheric exposure conditions and the specific paint/metal system in use. In various types of coatings, the epoxy zinc-rich coating attracts significant attention for its barrier property, mechanical property, excellent binding force with substrate, prominent resistance to water and chemical materials, etc. Hence, epoxy zinc-rich coating provides long-term protection for a metal substrate in a harsh environment and is used as anticorrosive primer in the marine environment.

Based on the above factors, this work aims to investigate the service life of epoxy zinc-rich coating which would be prolonged by the addition of Ni element in the steel. The mechanism of prolonging the coating service life of Ni element addition into steel was studied at the interface between steel and coating. 3 wt.% Ni-advanced (3Ni) low-alloy steel was independently explored by Shougang group to observe the interaction effect between the substrate and the coating. The role of the alloying elements and their distribution in the corrosion layers were observed by electron probe micro-analyzer technique (EPMA). The positive effect of protection for substrate was also tested in salt spray test for different time by electrochemical impedance spectroscopy (EIS).

## 2 Experimental

### 2.1 Materials and preparation

The chemical compositions of CS plate and 3Ni-advanced steel are shown in Table 1 which are supplied by Shougang group. The samples with a dimension of 150 mm × 75 mm × 3 mm were sandblasted followed by degreasing with acetone, and then epoxy zinc-rich primers were coated on CS and 3Ni-advanced steel substrates by brushes. The coated panels were cured at room temperature for one week prior to experiment. Coated samples were exposed using a glass tube fixed on the coating surface using an O-ring with an exposed surface area of 3.14 cm$^2$. The dry film thickness of paints was measured using an Elcometer 456 coating thickness gauge of 100 ± 20 μm.

### 2.2 Corrosion protection evaluation

The salt spray test (SST) was carried out to simulate the marine atmosphere environment according to ASTM B117. The solution of 5.0 wt.% NaCl (pH of 7.0) was added and vaporized into a salt spray at 40 °C in a salt spray chamber. The scratched line of coated panels (50 mm × 2 mm) was prepared by a surgical knife according to ISO 12944-6 and exposed to salt fog for certain time. Adhesive strength of coatings on the substrate was measured using an automatic adhesion tester (PosiTest AT-A, DeFelsko, USA).

EIS was tested on the surface of coating system after salt spray test for different time. A conventional three-electrode system was used which consisted of a Pt counter electrode, an Ag/AgCl reference electrode and the coated steel plate as working electrode (with an exposed area of 3.14 cm$^2$). All tests were carried out on a Parstat 4000 electrochemical workstation (Princeton Applied Research, USA) by varying the measured frequency from 100 kHz to 0.01 Hz at open-circuit potential with an alternating current perturbation of 20 mV sinusoidal voltage (peak-to-zero) in 3.5 wt.% NaCl solution at room temperature.

**Table 1** Chemical compositions of Q345 steel and 3Ni-advanced steel (wt.%)

| Material | C | Si | Mn | P | S | Ni | Cu | Fe |
|---|---|---|---|---|---|---|---|---|
| Q345 | 0.01–0.05 | 0.1–0.3 | 0.5–1.0 | 0.001–0.004 | 0.001–0.003 | – | – | Balance |
| 3Ni | 0.01–0.05 | 0.1–0.3 | 0.5–1.0 | 0.001–0.004 | 0.001–0.003 | 3 | 0.1–0.5 | Balance |

## 2.3 Characterization

The morphologies of metallographic structure of CS and 3Ni steel were characterized by inverted metallurgic microscopy (Leica DMI500M, Germany). The scanning electron microscope (SEM, S-3400 N) was used to observe the cross-section morphology of coated steel after aging experiment of salt fog. Element distribution of corrosion products at the interface between coating and metal matrix was obtained by EPMA (EPMA-1720, SHIMADZU, Japan). Power X-ray diffraction (XRD) was taken on a Bruker D8 Advance analyzer at a range of 20°–105° with a scanning rate of 2 (°)/min and scanning step of 0.03° to characterize the crystalline phases of the corrosion products. The parameters of the generator were set as 40 kV and 150 mA.

## 3 Results and discussion

### 3.1 Microstructural characterizations of CS and 3Ni steel

Figure 1 shows representative micrographs of CS and 3Ni-advanced steel. Equiaxial grain ferrite and granular bainite microstructures of CS steel are presented in Fig. 1a. Meanwhile, the blank of fragmented cementite is present along the grain boundary. The advanced WS with the nickel content of 3 wt.% also shows the presence of ferrite microstructures in Fig. 1b, and the grain size is larger than that of CS. It is found that the order of corrosion resistance for different phase organizations is as follow: $R_{ct}$ (ferrite) $> R_{ct}$ (bainite) $> R_{ct}$ (pearlite) ($R_{ct}$ is charge transfer resistance) [32]. In Fig. 1b, it has been proven that the corrosion resistance of 3Ni steel is better than that of carbon steel for the presence of ferrite microstructures in 3Ni steel.

## 3.2 Anticorrosive performance of coating

Defects in organic coatings may originate from the production process (e.g., cutting edges and forming induced defects) or from mechanical scratch. Moreover, coatings may possess ionic conductive pathways which located at the interface, so that the corrosion starts at sites of the coating inducing invisible damage. Meanwhile, the scratched coating can be used to evaluate the corrosion protection of coating rapidly. Figure 2 shows surface morphology of scratched coating after different salt spray time. Figure 2a, b shows the morphology for the substrate of CS, and Fig. 2c, d shows the morphology for 3Ni steel substrate in the experiment time of 84 and 120 days. It is obviously that the width of corrosion extends with time along the scratched line. Moreover, the width of coated 3Ni steel is lower than that of the coated CS. Thus, the coated CS endured aggressive corrosion in the scratched zone, while the coated 3Ni steel endured lower corrosion attack and had most intact surface in the scratched zone. It is due to the fact that 3Ni steel substrate was better anticorrosive than CS [23, 33].

### 3.3 Rust layer characteristic and elemental distribution

The cross-section images of scratched coating with corrosion product on CS and 3Ni steel are shown in Fig. 3. In general, the rust layer is thick for CS and the thickness grew gradually with the corrosion proceeding as shown in Fig. 3a and b. It can be found that the rust layer is not dense, and there are some cracks and porous structure. However, in Fig. 3c and d, the rust layer is dense and there are little cracks for 3Ni steel; the thickness of the rust layer does not increase significantly with experiment time. As a consequence, it can be concluded that the surface products on 3Ni steel are more compact than those on CS, which
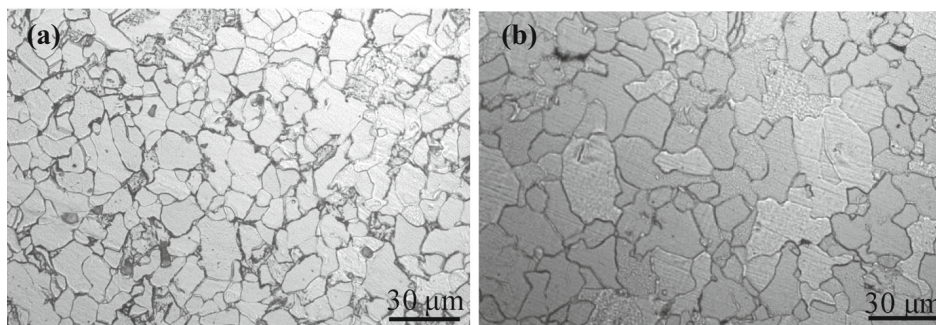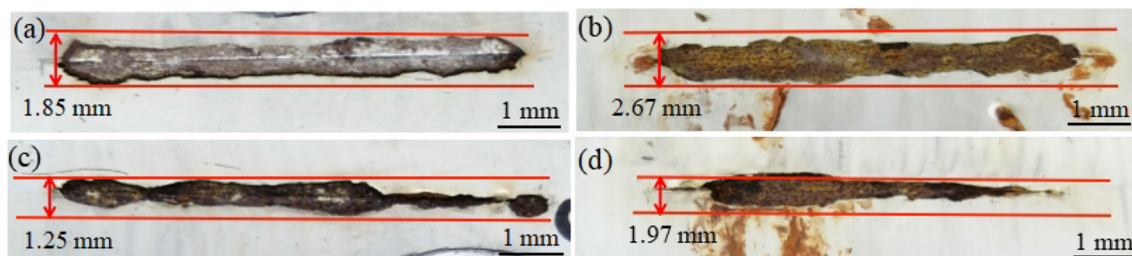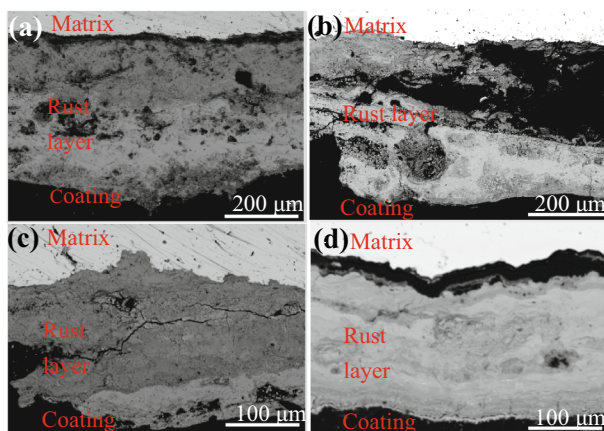


**Fig. 1** Metallographic microstructures of CS (**a**) and 3Ni steel (**b**)

**Fig. 2** Surface morphology of scratched coating after salt spray for different time of CS (**a**, **b**) and 3Ni steel (**c**, **d**). **a**, **c** 84 days; **b**, **d** 120 days



**Fig. 3** Cross-section images of scratched coating with corrosion product after different time of salt spray test in CS (**a**, **b**) and 3Ni steel (**c**, **d**). **a**, **c** 42 days; **b**, **d** 84 days

could be better resistant to the invasion of electrolyte in marine atmosphere.

Element mappings of the corrosion product are shown in Fig. 4. The chloride and nickel concentration is shown in the rust layer. In Fig. 4a, Cl element distributes as the band pattern in the inner rust layer of CS for the time of 42 days, and the content of Cl element is between 1.72% and 6.34%. However, the content of Cl is about 1.72% or lower to 1.72% to 3Ni steel in Fig. 4c. Cl element mainly locates in the outer rust layer, and the concentration of Cl element in 3Ni steel is obviously lower than that of CS. Following the aging time of 84 days in Fig. 4b, the rust layer of CS generally shows a uniform chloride ingress from the top surface to inside of product film, and the proportion of Cl is between 1.53% and 3% (Fig. 4b). Similarly, Cl element ingresses into the inner layer of rust with aging time of 3Ni steel (Fig. 4d) and content is about 1.53%. As stated, the concentration of Cl element for 3Ni steel is obviously lower than that of CS. It is ascribe to forming the dense and compact corrosion product layers in 3Ni steel, preventing the enrichment of chloride ions. Simultaneously, Ni element is also detected in the rust layer of coated 3Ni steel (Fig. 4e, f). As shown in Fig. 4e, Ni element uniformly distributes in the rust layer from the top surface to inside of

product film and the proportion is about 6.49% in the aging time 42 days. However, in the long aging time, Ni element is enriched in the outer layer of rust as a line of banding and the content increases to be about 15% (Fig. 4f), which is approximate two and a half times that of CS.
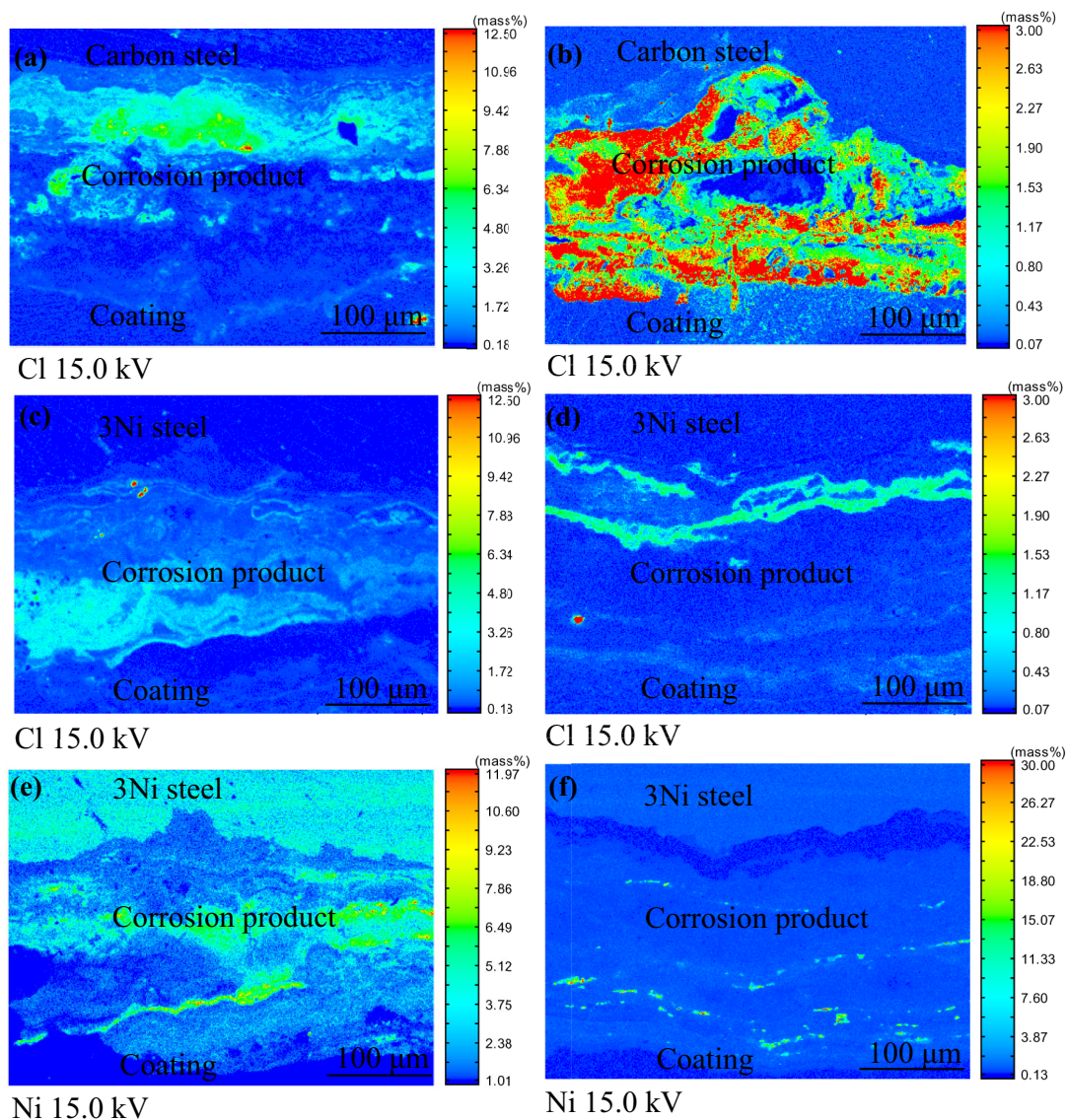
### 3.4 Compositions of corrosion product

XRD patterns for the corrosion products under the scratched coat on CS and 3Ni steel after salt spray tests for 84 days are shown in Fig. 5. The results display the same compositions of ferric oxyhydroxides on the coated carbon steel and 3Ni steel, including lepidocrocite ($\gamma$-FeOOH) and $Fe(OH)_3$. However, it is also found that $NiFe_2O_4$ and $Fe_2O_3$ appeared in the corrosion product of 3Ni steel. Wu et al. [33] reported that $NiFe_2O_4$ in the product film can refine the grains of ferric oxides and ferric oxyhydroxides, and improve the structure of the products, resulting in a dense and crack-free film tightly adhered to the metal substrate.

### 3.5 EIS measurement

EIS measurement can be used to study the corrosion protective properties of organic coatings on the metal surface. The primary consideration is the corrosion occurrence on the metal/coating interface happened [31, 34]. Figure 6 shows Nyquist and Bode diagrams of EIS results for CS and 3Ni steel in salt spray test for different time. $Z_{re}$ is the real part of impedance, $Z_{im}$ is the imaginary part of impedance, and $|Z|$ is the impedance modulus of value. In Fig. 6a and c, it is obviously that the radius of capacitive arc for 3Ni steel are larger than that of CS, which means that the substrate of nickel steel can improve the protection ability and prolong the failure time of coating.

The impedance modulus of $|Z|$ at the low frequency of 0.01 Hz ($|Z|_{0.01}$) can be used to evaluate the protective effect of coating [35, 36]. The change of impedance modulus at the low frequency ($f = 0.01$ Hz) of the zinc-rich coating on steel surface for different salt spray time is given in Fig. 7. As show in Fig. 7, the protection of coating for CS matrix is divided into three stages with delayed time. In stage I, the zinc powders of coating were corroded

**Fig. 4** Images distribution of elements Cl (**a–d**) and Ni (**e, f**) in corrosion product for CS (**a, b**) and 3Ni steel (**c–f**) after different test time observed by EPMA. **a, c, e** 42 days; **b, d, f** 84 days
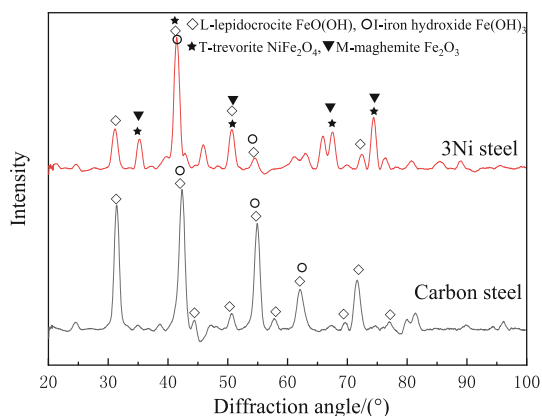


**Fig. 5** Phase compositions of corrosion products under scratched coating after salt spray tests for 84 days

in the initial time of salt spray test and the modulus $|Z|_{0.01}$ declined. In stage II, barrier protection provided by the epoxy primer and corrosion product with self-dissolution of zinc provided by the zinc particles led to the increase in modulus $|Z|_{0.01}$. At the final stage III, the protection of coating was destroyed by corrosive medium of $Cl^-$ and modulus $|Z|_{0.01}$ declined below the value of $10^5 \ \Omega \ cm^2$, it is suggested that the protection effect of coatings decreases and the coating gradually fails [37, 38]. Similarly, the modulus $|Z|_{0.01}$ of 3Ni steel decreased from 0 to 400 h for the corrosion of zinc. However, the value of $|Z|_{0.01}$ increased above the value of $10^5 \ \Omega \ cm^2$ for the barrier protection in following time resulted in better binding force between 3Ni steel substrate and coating. It is suggested that the positive effect of 3Ni steel imposed on the coating
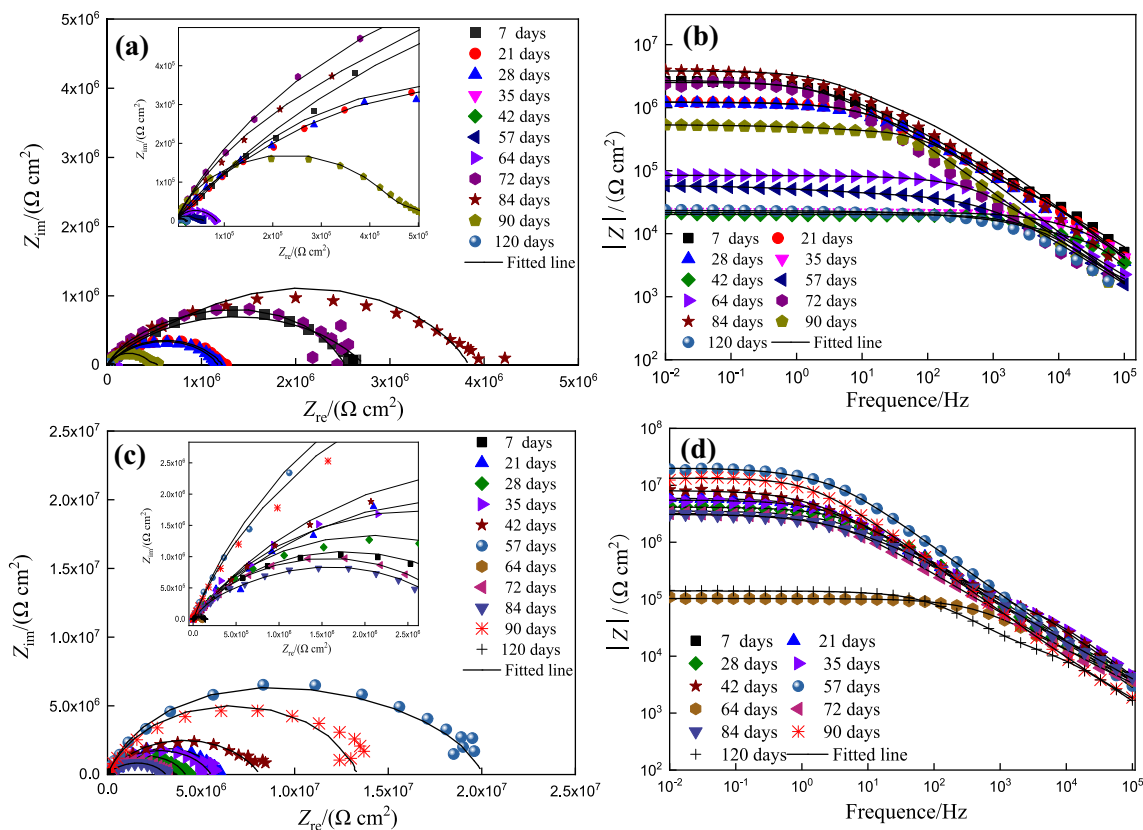
**Fig. 6** Nyquist (**a**, **c**) and Bode plots (**b**, **d**) of EIS results for CS (**a**, **b**) and 3Ni steel (**c**, **d**) in different salt spray time
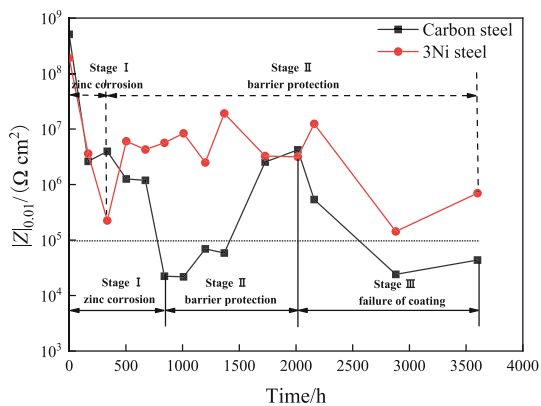


**Fig. 7** Change of impedance modulus at low frequency ($f = 0.01$ Hz) of zinc rich coating on steel surface after salt spray test for different time



**Fig. 8** Equivalent circuit model used to fit experiment impedance data of CS and 3Ni steel

CPE was used to replace the capacitance to achieve a better fitting result. $n$ ($0 < n < 1$) is the coefficient of dispersion which denotes the deviation between the double-layer capacitance of solid electrode and the pure capacitance. The fitting results of CS and 3Ni steel in different time are shown in Tables 2 and 3.

The variation of $CPE_2$ of zinc corrosion with salt spray experiment for CS and 3Ni steel are shown in Fig. 9a. As shown, $CPE_2$ of CS increases from $1.39 \times 10^{-9}$ to $3.63 \times 10^{-6}$ F cm$^{-2}$ s$^{-n}$, and then decreases rapidly in the following time. However, the trend of 3Ni steel is flatted during the experiment time and lower than that of CS. It is suggested that more dielectric medium is contained in the corrosion product of coated CS with zinc particles. Furthermore, the similar trend of $R_t$ for CS and 3Ni steel are shown in Fig. 9b. As shown in Fig. 9b, the value of $R_t$ of 3Ni steel is higher than that of CS in the initial and final

protection. Therefore, the substrate of 3Ni steel had beneficial effect for prolonging the service life of coating.

The equivalent circuit model is shown in Fig. 8 and is employed to fit the results of EIS spectra. In Fig. 8, $R_s$ is the solution resistance, $CPE_1$ is the capacitance of coating, and $R_c$ is the pore resistance of coating. $CPE_2$ and $R_t$ represent the double layer capacitance and charge transfer resistance of production for zinc corrosion, respectively. Considering the depression effect, a constant phase element
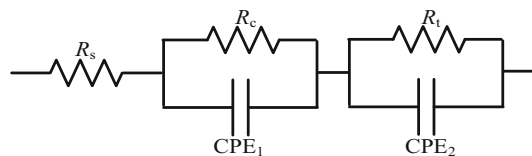
**Table 2** $R$, CPE and $n$ values obtained from fitting of EIS for zinc rich epoxy coating on Q345 steel in different time

| Time/day | $CPE_1/(S\ cm^{-2}\ s^{-n})$ | $n_1$ | $R_c/(\Omega\ cm^2)$ | $CPE_2/(S\ cm^{-2}\ s^{-n})$ | $n_2$ | $R_t/(\Omega\ cm^2)$ |
|---|---|---|---|---|---|---|
| 7 | $5.28 \times 10^{-8}$ | 0.61 | $2.74 \times 10^6$ | – | – | – |
| 21 | $3.51 \times 10^{-8}$ | 0.68 | $1.21 \times 10^6$ | $1.39 \times 10^{-9}$ | 1.00 | $1.63 \times 10^4$ |
| 28 | $4.11 \times 10^{-8}$ | 0.74 | $8.07 \times 10^4$ | $3.83 \times 10^{-8}$ | 0.7 | $1.09 \times 10^6$ |
| 35 | $7.72 \times 10^{-10}$ | 0.98 | $9.04 \times 10^3$ | $2.41 \times 10^{-8}$ | 0.77 | $1.27 \times 10^4$ |
| 42 | $5.93 \times 10^{-10}$ | 1.00 | $7.24 \times 10^3$ | $3.5 \times 10^{-8}$ | 0.80 | $1.30 \times 10^4$ |
| 57 | $1.56 \times 10^{-5}$ | 0.51 | $1.74 \times 10^4$ | $7.42 \times 10^{-8}$ | 0.68 | $4.06 \times 10^4$ |
| 64 | $1.71 \times 10^{-8}$ | 0.95 | $2.52 \times 10^4$ | $1.27 \times 10^{-7}$ | 0.62 | $5.91 \times 10^4$ |
| 72 | $2.84 \times 10^{-8}$ | 0.76 | $1.66 \times 10^6$ | $6.59 \times 10^{-8}$ | 0.82 | $8.65 \times 10^5$ |
| 84 | $2.98 \times 10^{-8}$ | 0.72 | $3.38 \times 10^6$ | $1.37 \times 10^{-8}$ | 0.77 | $4.67 \times 10^5$ |
| 90 | $1.18 \times 10^{-8}$ | 0.81 | $4.48 \times 10^5$ | $3.63 \times 10^{-6}$ | 0.63 | $8.67 \times 10^4$ |
| 120 | $2.63 \times 10^{-6}$ | 0.58 | $6.73 \times 10^3$ | $1.91 \times 10^{-8}$ | 0.78 | $1.65 \times 10^4$ |

$n_1$, $n_2$ Dispersion coefficient of double-layer capacitance for coating and zinc corrosion products, respectively

**Table 3** $R$, CPE and $n$ values obtained from fitting of EIS for zinc rich epoxy coating on 3Ni steel in different time

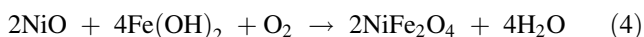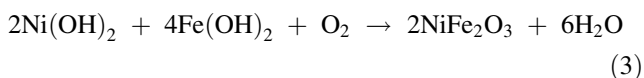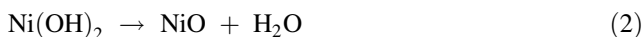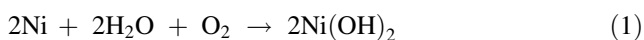| Time/day | $CPE_1/(S\ cm^{-2}\ s^{-n})$ | $n_1$ | $R_c/(\Omega\ cm^2)$ | $CPE_2/(S\ cm^{-2}\ s^{-n})$ | $n_2$ | $R_t/(\Omega\ cm^2)$ |
|---|---|---|---|---|---|---|
| 7 | $1.18 \times 10^{-9}$ | 1.00 | $3.73 \times 10^3$ | $2.93 \times 10^{-8}$ | 0.70 | $3.55 \times 10^6$ |
| 21 | $5.81 \times 10^{-8}$ | 0.66 | $5.59 \times 10^5$ | $2.68 \times 10^{-8}$ | 0.77 | $5.37 \times 10^6$ |
| 28 | $2.27 \times 10^{-9}$ | 1.00 | $1.41 \times 10^3$ | $2.04 \times 10^{-8}$ | 0.73 | $4.16 \times 10^6$ |
| 35 | $1.44 \times 10^{-9}$ | 0.89 | $5.56 \times 10^6$ | $2.11 \times 10^{-8}$ | 0.71 | $8.19 \times 10^4$ |
| 42 | $2.72 \times 10^{-8}$ | 0.71 | $8.11 \times 10^6$ | $1.35 \times 10^{-9}$ | 1.00 | $3.38 \times 10^4$ |
| 57 | $6.49 \times 10^{-9}$ | 0.84 | $1.17 \times 10^7$ | $4.52 \times 10^{-8}$ | 0.76 | $8.41 \times 10^6$ |
| 64 | $9.52 \times 10^{-10}$ | 0.99 | $2.95 \times 10^3$ | $3.13 \times 10^{-8}$ | 0.72 | $1.00 \times 10^5$ |
| 72 | $4.17 \times 10^{-8}$ | 0.68 | $3.22 \times 10^6$ | $6.38 \times 10^{-5}$ | 0.99 | $1.87 \times 10^5$ |
| 84 | $2.47 \times 10^{-8}$ | 0.97 | $1.33 \times 10^5$ | $4.64 \times 10^{-8}$ | 0.64 | $2.98 \times 10^6$ |
| 90 | $4.51 \times 10^{-9}$ | 0.87 | $2.22 \times 10^7$ | $2.42 \times 10^{-8}$ | 0.85 | $4.38 \times 10^7$ |
| 120 | $1.02 \times 10^{-8}$ | 0.86 | $7.76 \times 10^3$ | $6.28 \times 10^{-8}$ | 0.76 | $1.32 \times 10^5$ |
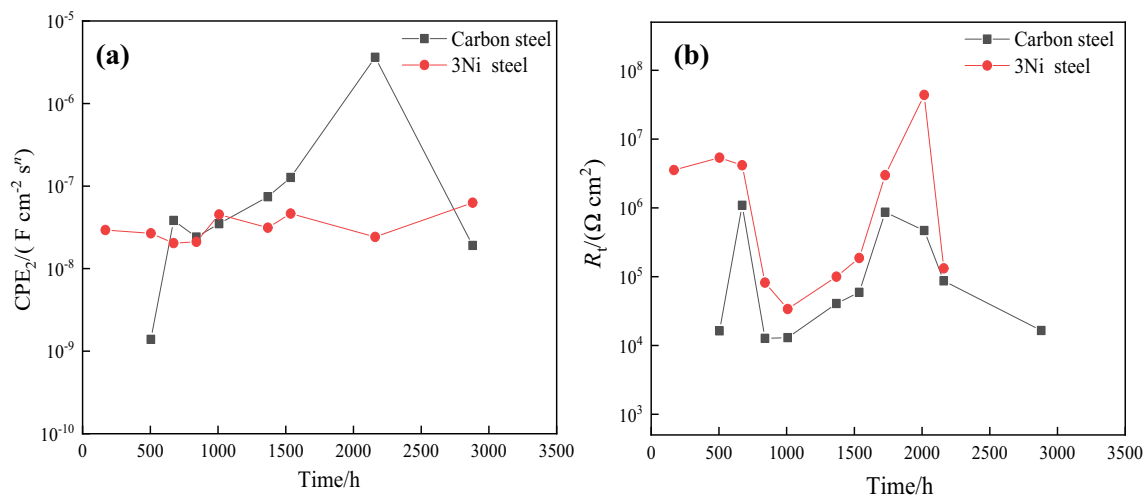


**Fig. 9** Change of $CPE_2$ (**a**) and $R_t$ (**b**) of zinc corrosion after different time of salt spray test

periods of the experiment. In conclusion, the substrate of 3Ni steel is helpful to form the better protection of zinc corrosion in the coating and prolong the service life of coating.

## 3.6 Discussion

SEM images (Fig. 3a–d) indicated that the uniform rust layer on 3Ni steel was much thinner than that on CS. Moreover, the rust layer was very compact, and tightly adhered to the substrate of 3Ni steel. However, the product layer on CS presented many cracks and pores which were even located close to the substrate. Accordingly, the outside of corrosive medium may easily get through the product film and further damage the metal substrate by means of these cracks and pores. As shown in Fig. 4a–d, this evidence was confirmed by the distribution of Cl, which was significantly concentrated in the loose and cracked areas. Furthermore, as indicated in Fig. 4c–f, Cl-rich region precisely corresponds to Ni poor region, and it was suggested that a repulsive interaction existed between Ni and Cl in the product film.

According to the published papers [19, 39], Ni was present in the corrosion product worked as a bivalent state. Ni atoms can participate in the corrosion process at the early stage and a small amounts of $Ni(OH)_2$ and NiO were formed in the product film. Kimura et al. [40] referred that $Ni^{2+}$ could substitute $Fe^{2+}$ at octahedral sites of $Fe_3O_4$ to form a $NiFe_2O_4$ phase in the products. Hou et al. [41] reported that $NiFe_2O_4$ was more thermodynamically stable than $Fe_3O_4$, and could be generated by the reaction of precipitation between $Fe(OH)_2$ and $Ni(OH)_2$ [42, 43]. Thus, it can be concluded that the scattered $Ni(OH)_2$ and NiO in the original product film can react with $Fe(OH)_2$, leading to the formation of the spinel phase $NiFe_2O_4$ in the corrosion product layer. The relevant chemical reactions are as follows [33]:

$$2Ni + 2H_2O + O_2 \rightarrow 2Ni(OH)_2 \tag{1}$$

$$Ni(OH)_2 \rightarrow NiO + H_2O \tag{2}$$

$$2Ni(OH)_2 + 4Fe(OH)_2 + O_2 \rightarrow 2NiFe_2O_3 + 6H_2O \tag{3}$$

$$2NiO + 4Fe(OH)_2 + O_2 \rightarrow 2NiFe_2O_4 + 4H_2O \tag{4}$$

Generally, the corrosion resistance of substrate and the coating determined the service life of a coated steel in a marine atmosphere. In our investigation, the coated 3Ni steel displayed a better resistance to atmospheric corrosion than coated CS in tropical marine environment (Figs. 6 and 7). There is no doubt that this improvement of resistance was attributed to the addition of Ni to the steel. The granular $Ni(OH)_2$, NiO, and $NiFe_2O_4$ can refine the grains

of ferric oxides and ferric oxyhydroxides in the product, improve the structure of the products, meanwhile evolve a dense and crack-free film and be tightly adhered to the metal substrate as shown in Fig. 3. As a result, the corrosive medium including chloride ion was effectively blocked to reach the substrate. Some research reported that corrosion product film of Ni steel possessed cation selectivity owing to the spinel phase of $NiFe_2O_4$ [23, 44]. Consequently, the chloride ions can be obstructed into the inside products and weaken the localized acidification effect from autocatalysis of chloride ion in the products. For the presence of oxygen and oxygen reduction occurred below the defect of organic coating, an alkaline pH was formed during the oxygen reduction and a passive iron surface in an alkaline area would generate [39]. Therefore, the addition of nickel can also reduce the local acidification caused by chloride ions and protect the passive layer of corrosion product.

## 4 Conclusion

The corrosion behavior of intact and defective coatings for coated CS and 3Ni steel exposed to a marine atmosphere was systematically analyzed by various techniques. The coated 3Ni steel displayed a better resistance to atmospheric corrosion than coated CS in tropical marine environment. When the coating was broken, the expansion rate of corrosion for 3Ni steel under the coating was slower than that for CS, leading to prolonging the service life of the coated 3Ni steel. It was also found that $NiFe_2O_4$ and $Fe_2O_3$ appeared in the corrosion product of 3Ni steel, and $NiFe_2O_4$ can refine the grains of corrosion products. The addition of Ni element in the substrate steel can improve the protection of coating and a dense with little cracks film of product generated and was tightly adhered to the metal substrate. Chloridion can be obstructed into the inside products by the enrichment of Ni element in rust layer.

## References

[1] M. Morcillo, I. Díaz, H. Cano, B. Chico, D. de la Fuente, Constr. Build. Mater. 213 (2019) 723–737.

[2] M. Morcillo, I. Díaz, H. Cano, B. Chico, D. de la Fuente, Constr. Build. Mater. 222 (2019) 750–765.

[3] L. Hao, S.X. Zhang, J.H. Dong, W. Ke, Corros. Sci. 58 (2012) 175–180.

[4] Z.M, Cuo. Y.L. Chen, Z.L. Mi, Y.D. Wang, H.T. Jiang, J. Iron Steel Res. Int. 26 (2019) 1000–1010.

[5] S.S. Liu, H.Y. Chen, X. Zhao, L. Fan, X.M. Guo, Y.S. Yin, J. Iron Steel Res. Int. 26 (2019) 191–199.

[6] L.L. Zhao, K. Xiao, C.F. Dong, X.Q. Cheng, W. Xue, W. Yu, J. Iron Steel Res. Int. 26 (2019) 1315–1328.

[7] Q.Y. Zang, Y.F. Jin, T. Zhang, Y.Y. Tao, J. Iron Steel Res. Int. 27 (2020) 451–460.

[8] Y.T. Ma, Y. Li, F.H. Wang, Corros. Sci. 51 (2009) 1725–1732.

[9] I. Sugimoto, K. Kita, Quart. Rep. RTRI 51 (2010) 33–37.

[10] T. Ishikawa, M. Kumagai, A. Yasukawa, K. Kandori, T. Nakayama, F. Yuse, Corros. Sci. 44 (2002) 1073–1086.

[11] T. Nishimura, H. Katayama, K. Noda, T. Kodama, Corros. Sci. 42 (2000) 1611–1621.

[12] Y. Zhou, J. Chen, Y. Xu, Z. Liu, J. Mater. Sci. Technol. 29 (2013) 168–174.

[13] G.Q. Fu, M.Y. Zhu, X.L. Gao, Mater. Sci. 22 (2016) 501–505.

[14] T. Murata, Weathering steel, in: R.W. Revie (Eds.), Uhlig'S Corrosion Handbook, John Wiley and Sons, Inc., New York, USA, 2000.

[15] L.Y. Song, Z.Y. Chen, B.R. Hou, Corros. Sci. 93 (2015) 191–200.

[16] J.S. Wang, P.Y. Shi, L.J. Chen, M.F. Jiang, J. Iron Steel Res. Int. 22 (2015) 1020–1023.

[17] J.H. Jia, W. Wu, X.Q. Cheng, J.B. Zhao, Constr. Build. Mater. 245 (2020) 118463.

[18] X.Q. Cheng, Y.W. Tian, X.G. Li, C. Zhou, Mater. Corros. 65 (2014) 1033–1037.

[19] I. Diaz, H. Cano, D. de la Fuente, B. Chico, J.M. Vega, M. Morcillo, Corros. Sci. 76 (2013) 348–360.

[20] H. Cano, D. Neff, M. Morcillo, P. Dillmann, I. Diaz, D. de la Fuente, Corros. Sci. 87 (2014) 438–451.

[21] X.H. Chen, J.H. Dong, E.H. Han, W. Ke, Can. Metall. Quart. 46 (2007) 195–206.

[22] Q. Yu, C.F. Dong, Y.H. Fang, K. Xiao, C.Y. Guo, G. He, X.G. Li, J. Iron Steel Res. Int. 23 (2016) 1061–1070.

[23] X.Q. Cheng, Z. Jin, M. Liu, X.G. Li, Corros. Sci. 115 (2017) 135–142.

[24] S.J. Travassos, M.B. Almeida, C.R. Tomachuk, H.G. de Melo, J. Mater. Res. Technol. 9 (2020) 687–699.

[25] M.H. Sun, C.W. Du, Z.Y. Liu, C. Liu, X.G. Li, Y.M. Wu, Corros. Sci. 186 (2021) 109427.

[26] Y. Qiang, S. Zhang, B. Tan, S. Chen, Corros. Sci. 133 (2018) 6–16.

[27] L.M. Calado, M.G. Taryba, M.J. Carmezim, M.F. Montemor, Corros. Sci. 142 (2018) 12–21.

[28] Y. He, I. Dobryden, J. Pan, A. Ahniyaz, T. Deltin, R.W. Corkery, P.M. Claesson, Appl. Surf. Sci. 457 (2018) 548–558.

[29] Z. Mahidashti, T. Shahrabi, B. Ramezanzadeh, Prog. Org. Coat. 114 (2018) 19–32.

[30] R. Jain, R. Pitchumani, Surf. Coat. Technol. 337 (2018) 223–231.

[31] S.G. Zhou, Y.M. Wu, W.J. Zhao, J.J. Yu, F.W. Jiang, Y.H. Wu, L.Q. Ma, Mater. Des. 169 (2019) 107694.

[32] Y. Zhang, F. Huang, Q. Hu, Z.X. Peng, J. Liu, Mater. Chem. Phys. 241 (2020) 122045.

[33] W. Wu, X.Q. Cheng, H.X. Hou, B. Liu, X.G. Li, Appl. Surf. Sci. 436 (2018) 80–89.

[34] F.T. Shirehjini, I.D.H. Eskandari, D. Zarei, J. Mater. Sci. Technol. 32 (2016) 1152–1160.

[35] X. Ma, L.K. Xu, W. Wang, Z.F. Lin, X.B. Li, Corros. Sci. 120 (2017) 139–147.

[36] A. Amirudin, D. Thieny, Prog. Org. Coat. 26 (1995) 1–28.

[37] Y. Cubides, H. Castaneda, Corros. Sci. 109 (2016) 145–161.

[38] G. Bierwagen, D. Tallman, J. Li, L. He, C. Jeffcoate, Prog. Org. Coat. 46 (2003) 148.

[39] G. Grundmeier, W. Schmidt, M. Stratmann, Electrochim. Acta 45 (2000) 2515–2533.

[40] M. Kimura, H. Kihira, N. Ohta, M. Hashimoto, T. Senuma, Corros. Sci. 47 (2005) 2499–2509.

[41] Q. Hou, Z.Y. Liu, C.T. Li, X.G. Li, Appl. Surf. Sci. 426 (2017) 514–526.

[42] M. Sennour, L. Marchetti, F. Martin, S. Perrin, R. Molins, M. Pijolat, J. Nucl. Mater. 402 (2010) 147–156.

[43] X.Y. Zhong, E.H. Han, X.Q. Wu, Corros. Sci. 66 (2013) 369–379.

[44] X.H. Chen, J.H. Dong, E.H. Han, W. Ke, Mater. Lett. 61 (2007) 4050–4053.